Characterization of the Praesepe Star Cluster by Photometry and Proper Motions With 2MASS, PPMXL, and Pan-STARRS

Citation

Published Version

Permanent link

Terms of Use

Share Your Story

Characterization of the Praesepe Star Cluster by Photometry and Proper Motions with 2MASS, PPMXL, and Pan-STARRS

P. F. Wang[1], W. P. Chen[1,2], C. C. Lin[2], A. K. Pandey[3], C. K. Huang[2], N. Panwar[2],

C. H. Lee[2], M. F. Tsai[4], C.-H. Tang[4], B. Goldman[5], W. S. Burgett[6], K. C. Chambers[6],

P. W. Draper[7], H. Flewelling[6], T. Grav[8], J. N. Heasley[6], K. W. Hodapp[6], M. E. Huber[6],

R. Jedicke[6], N. Kaiser[6], R.-P. Kudritzki[6], G. A. Luppino[6], R. H. Lupton[9], E. A. Magnier[6],

N. Metcalfe[7], D. G. Monet[10], J. S. Morgan[6], P. M. Onaka[6], P. A. Price[6], C. W. Stubbs[11],

W. Sweeney[6], J. L. Tonry[6], R. J. Wainscoat[6], C. Waters[6]

[1]Department of Physics, National Central University, 300 Jhongda Road, Jhongli 32001, Taiwan

[2]Graduate Institute of Astronomy, National Central University, 300 Jhongda Road, Jhongli 32001, Taiwan

[3]Aryabhatta Research Institute of Observational Sciences, Manora Peak, Nainital 263129, India

[4]Department of Computer Science and Information Engineering, National Central University, 300 Jhongda Road, Jhongli 32001, Taiwan

[5]Max-Planck-Institut für Astronomie, Königstuhl 17, D-69117 Heidelberg, Germany

[6]Institute for Astronomy, University of Hawai'i, 2680 Woodlawn Drive, Honolulu HI 96822, USA

[7]Department of Physics, Durham University, South Road, Durham DH1 3LE, UK

[8]Department of Physics and Astronomy, Johns Hopkins University, 3400 North Charles Street, Baltimore, MD 21218, USA

[9]Department of Astrophysical Sciences, Princeton University, Princeton, NJ 08544, USA

[10]US Naval Observatory, Flagstaff Station, Flagstaff, AZ 86001, USA

[11]Department of Physics, Harvard University, Cambridge, MA 02138, USA

ABSTRACT

Membership identification is the first step to determine the properties of a star cluster. Low-mass members in particular could be used to trace the dynamical history, such as mass segregation, stellar evaporation, or tidal stripping, of a star cluster in its Galactic environment. We identified member candidates with stellar masses $\sim$0.11–2.4 $M_\odot$ of the intermediate-age Praesepe cluster (M 44), by using Pan-STARRS and 2MASS photometry, and PPMXL proper motions. Within a sky area of 3 deg radius, 1040 candidates are identified, of which 96 are new inclusions. Using the same set of selection criteria on field stars led to an estimate of a false positive rate 16%, suggesting 872 of the candidates being true members. This most complete and reliable membership list allows us to favor the BT-Settl model in comparison with other stellar models. The cluster shows a distinct binary track above the main sequence, with a binary frequency of 20–40%, and a high occurrence rate of similar mass pairs. The mass function is consistent with that of the disk population but shows a deficit of members below 0.3 solar masses. A clear mass segregation is evidenced, with the lowest-mass members in our sample being evaporated from this disintegrating cluster.

Subject headings: stars: kinematics and dynamics – stars: luminosity function, mass function — open clusters and associations: individual (Praesepe)

1. Introduction

A star cluster manifests itself as a density concentration of comoving stars in space. Born out of the same molecular cloud, the member stars have roughly the same age, similar chemical composition, and are at essentially the same distance from us. Star clusters, therefore, serve as good test beds to study stellar formation and evolution. In order to diagnose the properties of a star cluster, such as its age, distance, size, spatial distribution, mass function, etc., it is necessary to identify as completely as possible the member stars. In particular, with a sample of members including the lowest mass stars, or even substellar objects, one could trace the dynamical history of an open cluster, e.g., the effect of mass segregation, stellar evaporation, and tidal stripping in the Galactic environment.

Nearby open clusters are useful in study of their low-mass population. Praesepe (M 44; NGC 2632; the Beehive Cluster) is such a rich ($\sim$ 1000 members) and intermediate-age (757 Myr; Gáspár et al. 2009) stellar aggregation in Cancer, as a member in the Hyades moving group (Eggen 1960), also called the Hyades supercluster. Compared to Praesepe, the Hyades cluster itself has a scattered main sequence in the color-magnitude diagram (CMD) because of the significant depth with respect to its distance. The advantages of studying stars in Praesepe are numerous. First, with a distance determination ranging from 170 pc (Reglero & Fabregat 1991) to 184 pc (An et al. 2007), the cluster is close enough to detect low-mass stars or even brown dwarfs. In this work, we adopted a distance 179 ± 2 pc (Gáspár et al. 2009), and metallicity [Fe/H]=0.16 (Carrera & Pancino 2011). Second, the proper motion (PM) of the cluster is distinct from that of the field stars, so contamination is minimized when identifying member stars. Third, in contrast to a star cluster at birth, for which the spatial distribution of members is governed by the parental cloud structure, the stellar distribution in an evolved cluster depends mainly on the interaction between members, from which we could investigate the dynamical evolution of the cluster.

Early PM measurements of Praesepe included the pioneering work by Klein Wassink (1927) to identify bright members within a 1-deg radius of the cluster center, and by Jones & Cudworth (1983) who extended the detection limit to $V \sim 17$ mag to include intermediate-mass members. Wang et al. (1995) combined early data and presented a list of nearly 200 PM members. Using PMs and photometry, Jones & Stauffer (1991) identified a list of member candidates from $V \sim 9$ to 18 mag within $2°$ of the cluster center. Using optical and infrared photometry, Williams et al. (1995) selected member candidates with mass $M > 0.08 M_\odot$ and concluded a mass function similar to the field, with no evidence of stellar evaporation. Wang et al. (2011) summarized the photometric surveys of Praesepe members down to the hydrogen-burning limit. Notably, Hambly et al. (1995a), with a limiting magnitude of $R \gtrsim 20$ mag, thereby reaching the stellar mass of ~ 0.1 M$_\odot$, derived a rising mass function toward the low-mass end, and presented evidence of mass segregation (Hambly et al. 1995b). With the Two Micron All Sky Survey (2MASS) and Digital Sky Survey data covering a sky area of 100 deg^2, Adams et al. (2002) extended the lower main sequence to 0.1 M$_\odot$, and determined the radial density profile of member stars. Kraus & Hillenbrand (2007) surveyed a sky area of 300 deg^2 to identify members by optical to infrared spectral energy distribution, and by PM measurements taken from UCAC2 for bright stars or calculated from USNO-B1 and SDSS positions, reaching almost into the brown-dwarf regime. Their sample of early-type stars is incomplete because of the bright limit of UCAC2, whereas for later-type members the incompleteness is caused by the detection limits of USNO-B1 and 2MASS. Recently Khalaj & Baumgardt (2013) used SDSS and PPMXL data to characterize the stellar members, including the mass segregation effect and binarity.

There have been efforts to identify brown dwarfs in Praesepe. Pinfield et al. (1997) covered one deg^2 down to $I \sim 21$ mag and identified 19 brown-dwarf candidates without spectral confirmation. Chappelle et al. (2005) presented deep optical and near-infrared

observations covering 2.6 deg^2 to a mass limit of 0.06 M$_\odot$. González-García et al. (2006) explored the central 0.6 deg radius region, reaching a limit of $i_{\rm SDSS} \sim 24.5$ mag corresponding to $\sim$0.05–0.13 M$_\odot$, and identified one substellar candidate. Boudreault et al. (2010) performed an optical I_c band and near-infrared J and K_s band photometric survey covering 3.1 deg^2 with detection limits of $I_c \sim 23.4$ mag and $J \sim 20.0$ mag, and found a handful of substellar candidates. The substellar census was augmented by Wang et al. (2011) who, using very deep optical (riz and Y-band) photometry of the central 0.59 deg^2 region of the cluster, identified a few dozen substellar member candidates. The first spectroscopically confirmed L dwarf member in Praesepe was secured by Boudreault & Lodieu (2013).

The stellar mass function of Praesepe was found to rise until 0.1 M$_\odot$ (Hambly et al. 1995b; Chappelle et al. 2005; Baker et al. 2010; Boudreault et al. 2010), in contrast to the Hyades, which have about the same age but are deficient of very low-mass stars and brown dwarfs. Possible explanations include different initial mass functions for the two clusters, or that Praesepe somehow did not experience as much dynamical perturbation in its environments (Bouvier et al. 2008). A recent study with the UKIRT Infrared Deep Sky Survey (UKIDSS) Galactic Clusters Survey derived a declining mass function toward lower masses (Boudreault et al. 2012). One of the aims of this work is to secure a sample of highly probable members to address this issue.

The spatial distribution of star in a cluster is initially governed by the structure in the parental molecular cloud. As a star cluster ages, gravitational scattering by stellar encounters results in mass segregation (Spitzer & Shull 1975); that is, massive stars tend to concentrate toward the center of the cluster, whereas lower mass stars, with a greater velocity dispersion, are distributed out to greater radii. For Praesepe, Hambly et al. (1995a) combined their observations, complete to $R \sim 20.0$ mag and $I \sim 18.2$ mag, with

those of Mermilliod et al. (1990) with $I \lesssim 12$ mag, to show a clear mass segregation effect. While brown dwarfs may have a preferred spatial distribution within a young star cluster (Caballero 2008), they tend to be distributed uniformly as the cluster evolves de la Fuente Marcos & de la Fuente Marcos (2000).

Observational attempts to find and characterize members in a star cluster often are sufficiently deep but limited in sky coverage, or cover wide areas but are restricted to only brighter (more massive) members. Studies with large sky coverages usually secure membership on the basis of photometry, lacking PM measurements for faint members. In this paper, we present photometric (2MASS and Pan-STARRS) and astrometric (PPMXL) diagnostics to select the member candidates in Praesepe. Our sample allows us to characterize the cluster including the binarity, its size, the mass function and the segregation effect. We describe the photometric and PM data in Section 2, and how we identified probable members in Section 3. The discussion is in Section 4, for which we compare our results with those in the literature. The binarity is discussed, and evidence of mass segregation and tidal stripping is presented. The paper ends with a short summary as Section 5.

2. Data Sources

Data used in this study include photometry and PM measurements within a 5-deg radius around the Praesepe center (R.A.=08$^\mathrm{h}$40$^\mathrm{m}$, Decl.= $+19°42'$, J2000). Archival data were taken from the 2MASS Point Sources Catalog, PPMXL, and Pan-STARRS. The 2MASS Point Source Catalog (Skrutskie et al. 2006) has the 10σ detection limits of $J \sim 15.8$ mag, $H \sim 15.1$ mag, and $K_s \sim 14.3$ mag, and saturates around 4–5 mag. The typical astrometric accuracy for the brightest unsaturated sources is about 70–80 mas. PPMXL is an all-sky merged catalog based on the USNO-B1 and 2MASS positions of 900

million stars and galaxies, reaching a limiting $V \sim 20$ mag (Roeser et al. 2010). The typical error is less than 2 milliarcseconds (mas) per year for the brightest stars with Tycho-2 (Høg et al. 2000) observations, and is more than 10 mas yr^{-1} at the faint limit.

Pan-STARRS (the Panoramic Survey Telescope And Rapid Response System) is a wide field (7 deg^2) imaging system, with a 1.8 m, f/4.4 telescope (Hodapp et al. 2004), equipped with a 1.4 giga-pixel camera (Tonry et al. 2008). The prototype (PS1), located atop Haleakala, Maui, USA (Kaiser et al. 2010), has been patrolling the entire sky north of $-30°$ declination since mid-2010. Repeated observations of the same patch of sky with a combination of g_{P1}, r_{P1}, i_{P1}, z_{P1}, and y_{P1} bands several times a month produce a huge inventory of celestial objects that vary in brightness or in position. Deep static sky images and catalog of stars and galaxies are also obtained. The PS1 filters differ slightly from those of the SDSS (Abazajian et al. 2009). The g_{P1} filter extends 20 nm redward of g_{SDSS} for greater sensitivity and lower systematics for photometric redshift estimates. SDSS has no corresponding y filter (Tonry et al. 2012a). The limiting magnitudes are $g_{P1} \sim 22.5$ mag, $r_{P1} \sim 22$ mag, $i_{P1} \sim 21.5$ mag, $z_{P1} \sim 21$ mag, and $y_{P1} \sim 19.5$ mag, with the saturation limit of ~ 14 mag. Upon completion of its 3.5 year mission by early 2014, PS1 will provide reliable photometry and astrometry. While incremental photometry of PS1 is available at the moment, the calibration of astrometry, hence the PM measurements, will need yet to tie down the entire sky, so no PS1 PM data were used here. The photometric analysis and calibration is described in Magnier et al. (2013). PS1 photometry for each detected object has measurements at multiple epochs, but for the work reported here only the average magnitude is used. In our study, we therefore made use of the 2MASS photometry for stars too bright for PS1, plus the PS1 photometry for faint stars, and the PPMXL PMs to select and characterize stellar member candidates. In matching counterparts in different star catalogues, one arcsecond was used as the coincidence radius among PPMXL, PS1, and 2MASS sources.

3.   Candidate Selection

Our membership diagnosis relies on grouping in sky position, in PMs, and along the isochrones appropriate for the cluster in the infrared and optical CMDs. The sources with 2MASS photometric uncertainties greater than 0.05 mag, roughly reaching $J \sim 15.2$ mag, $H \sim 14.6$ mag, and $K_s \sim 14.5$ mag, were removed from the sample. Candidacy was then further winnowed in the J versus $J - K_s$ CMD by including only objects with $J - K_s$ colors within 0.3 mag from the Padova isochrones (Marigo et al. 2008). This initial, wide range of colors allowed us not to adopt an *a priori* stellar evolutionary model, but in turn to put different models to test, as demonstrated below.

With the initial photometric sample, we then identified stars with PMs close to that of the cluster. Obviously the choice of the range is a compromise between the quality and the quantity of the candidate list. The optimal range was decided by how the cluster grouping is blended with the field. The PPMXL data toward Praesepe are shown in Figure 1. The PM distribution has two peaks, one for the cluster ($\mu_\alpha \cos \delta \approx -36.5 \, \mathrm{mas \, yr^{-1}}$, $\mu_\delta \approx -13.5 \, \mathrm{mas \, yr^{-1}}$) and the other for field stars ($\mu_\alpha \cos \delta \approx -4 \, \mathrm{mas \, yr^{-1}}$, $\mu_\delta \approx -3 \, \mathrm{mas \, yr^{-1}}$). The latter is the reflex Galactic motion of the Sun toward this particular line of sight. The average PM we adopted for the cluster is close to those listed by SIMBAD, $\mu_\alpha \cos \delta \approx -35.99 \pm 0.14 \, \mathrm{mas \, yr^{-1}}$, and $\mu_\delta \approx -12.92 \pm 0.14 \, \mathrm{mas \, yr^{-1}}$ (Loktin & Beshenov 2003). Naturally, around the peak of the cluster, the distribution is dominated by members, and away from the peak the contamination by field stars becomes prominent. In fact, Praesepe is among a few cases where the cluster's motion is clearly separated from that of the field, so the PM distribution exhibits a distinct secondary peak due to the cluster.

We exercised two levels of PM selection. First, a Gaussian function was fitted to the secondary (cluster) peak. Even through the distribution is known to be non-Gaussian
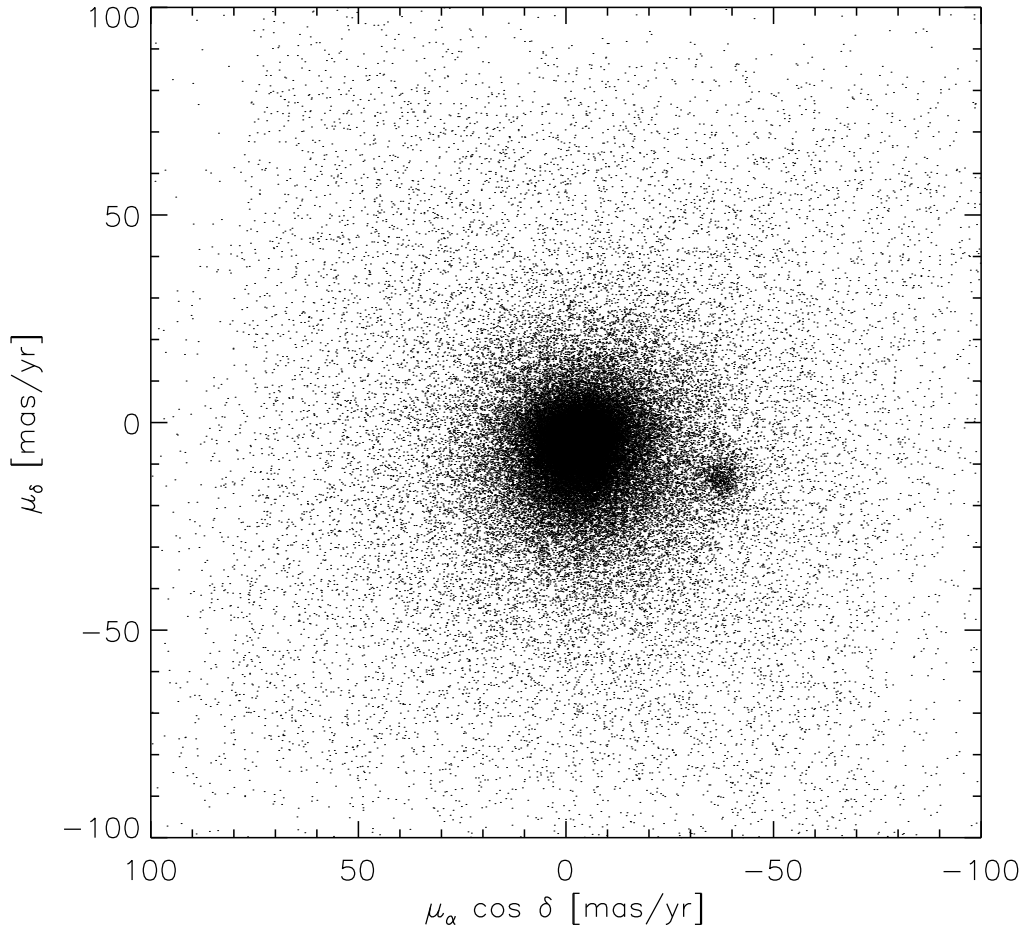
Fig. 1.— The PPMXL proper motion vector point diagram of stars toward Praesepe. Stars within an angular distance of 5° of the cluster center are analyzed. Only stars spatially within the central 2° are displayed here for clarity.

(Girard et al. 1989), the top part of the peak can be reasonably approximated by a Gaussian with a standard deviation of $9\,\mathrm{mas\,yr^{-1}}$. This is the PM range, namely within $\Delta\mu = 9\,\mathrm{mas\,yr^{-1}}$ of the cluster's average PM, that we adopted to select PM membership. This range is similar to that used by Kraus & Hillenbrand (2007) ($8\,\mathrm{mas\,yr^{-1}}$) or by Boudreault et al. (2012) ($8\,\mathrm{mas\,yr^{-1}}$ in $\Delta\mu_\alpha\cos\delta$ and $12\,\mathrm{mas\,yr^{-1}}$ in $\Delta\mu_\delta$). We note that Boudreault et al. (2012) derived, using relative PMs on the basis of the UKIDDS data, a different mean motion ($\mu_\alpha\cos\delta = -34.17 \pm 2.74\,\mathrm{mas\,yr^{-1}}$, $\mu_\delta = -7.36 \pm 4.17\,\mathrm{mas\,yr^{-1}}$). The discrepancy may arise because these authors used the median value to choose the center of the PM range, yet the distribution is skewed because of the contribution from the field. The next level of PM selection is $\Delta\mu = 4\,\mathrm{mas\,yr^{-1}}$, at which there is about the same contribution from the cluster and from the field, i.e., a 50% contamination of the sample. Figure 2 compares the cases of 4 versus $9\,\mathrm{mas\,yr^{-1}}$. While bright candidates, including giant stars, are not much affected by the choice, the cluster sequence clearly stands out with the narrower PM range even without restrictions on position, color, or magnitude. The adoption of $\Delta\mu < 9\,\mathrm{mas\,yr^{-1}}$ facilitates comparison between our results and previous works. But the $\Delta\mu < 4\,\mathrm{mas\,yr^{-1}}$ sample was still kept for a more reliable selection of candidates. Figure 2 also shows the PM distribution projected on the line connecting the peak of the field and the peak of the cluster. Even with this projection showing the maximum distinction between the two peaks, the distribution near the cluster is overwhelmed by that of the field.

Figure 3 shows the radial density profile of stars following roughly the cluster's isochrone and PM within the entire 5° field. The surface density decreases monotonically until around 3°, then levels off. Our analysis therefore was conducted within a spatial radius of 3°. At 179 pc, this corresponds to a linear dimension of ∼ 18 pc across. This size is relatively large among the 1657 entries with both angular diameter and distance
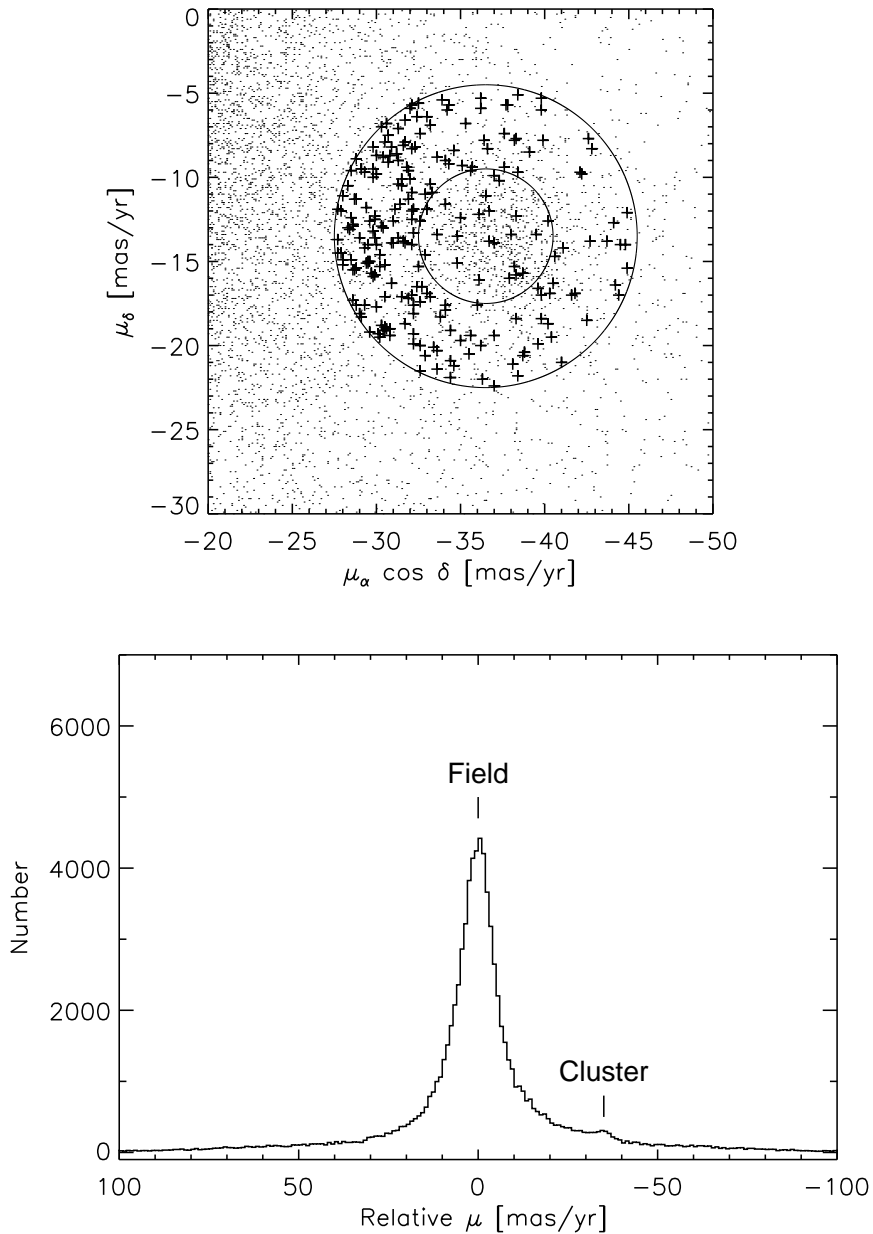
Fig. 2.— The 2MASS/PPMXL stars toward Praesepe. Top: The proper motion distribution. The two circles illustrate the cases of proper motion range of $\Delta\mu = 4$ mas yr^{-1} and of $\Delta\mu = 9$ mas yr^{-1}, respectively. Stars within $\Delta\mu = 9$ mas yr^{-1} but otherwise outside the cluster region (beyond 3°) and photometrically not following the cluster isochrone, i.e., field stars, are marked with crosses. Bottom: The projected PM distribution along the line connecting the field centroid and the cluster centroid. The bump near -35 mas yr^{-1} is due to the cluster, which has a standard deviation of 9 mas yr^{-1} when fitted with a Gaussian function.

determinations in the open cluster catalog compiled by Dias et al. (2002)[1], with the majority having diameters of 2–4 pc.

Figure 4 shows the J versus $J - K_s$ and the g_{P1} versus $g_{P1} - y_{P1}$ CMDs when the spatial (within or beyond 3° angular distance from the cluster center) and PM criteria (within 9 or $4 \, \mathrm{mas \, yr^{-1}}$) are applied. Even without a preselection by photometry or color, the cluster sequence is already evident. A subsample was chosen with a much restrictive set of parameters, namely with the angular distance within the central 30′, and with $\Delta\mu = 4$ mas yr^{-1}. This subsample is incomplete, but consists of highly secured members, which validates our initial rough selection ranges of magnitude and colors, and can be used to compare various stellar atmospheric models.

For the 2MASS/PPMXL sample, photometric candidacy is selected in the J versus $J - K_s$ CMD: (i) for stars brighter than $J \sim 12$ mag, from 0.06 mag below to 0.18 mag above and perpendicular to the Padova track; for giants there is no photometric restriction, i.e., only the spatial and kinematic criteria were applied; (ii) for fainter stars, from 0.1 mag below to 0.1 mag above and perpendicular to the Siess isochrone.

For stars fainter than the 2MASS sensitivity, we resorted to the PS1 data collected up to January 2012. The luminosity function toward Praesepe reaches beyond $g_{P1} \sim 21.5$ mag, but our data are limited by the sensitivity of the PPMXL dataset at around 21 mag. To avoid spurious detections, only sources that have been measured more than twice in both g_{P1} and y_{P1} bands were included in our analysis. The g_{P1} magnitudes were derived from the SDSS magnitudes (taken from Kraus & Hillenbrand 2007) transformed to the PS1 photometric system (Tonry et al. 2012a), namely, by $g_{p1} = g_{SDSS} - 0.012 - 0.139 \, x$, where $x = (g - r)_{SDSS}$. For the y_{P1} magnitudes, because SDSS has no corresponding y,

---

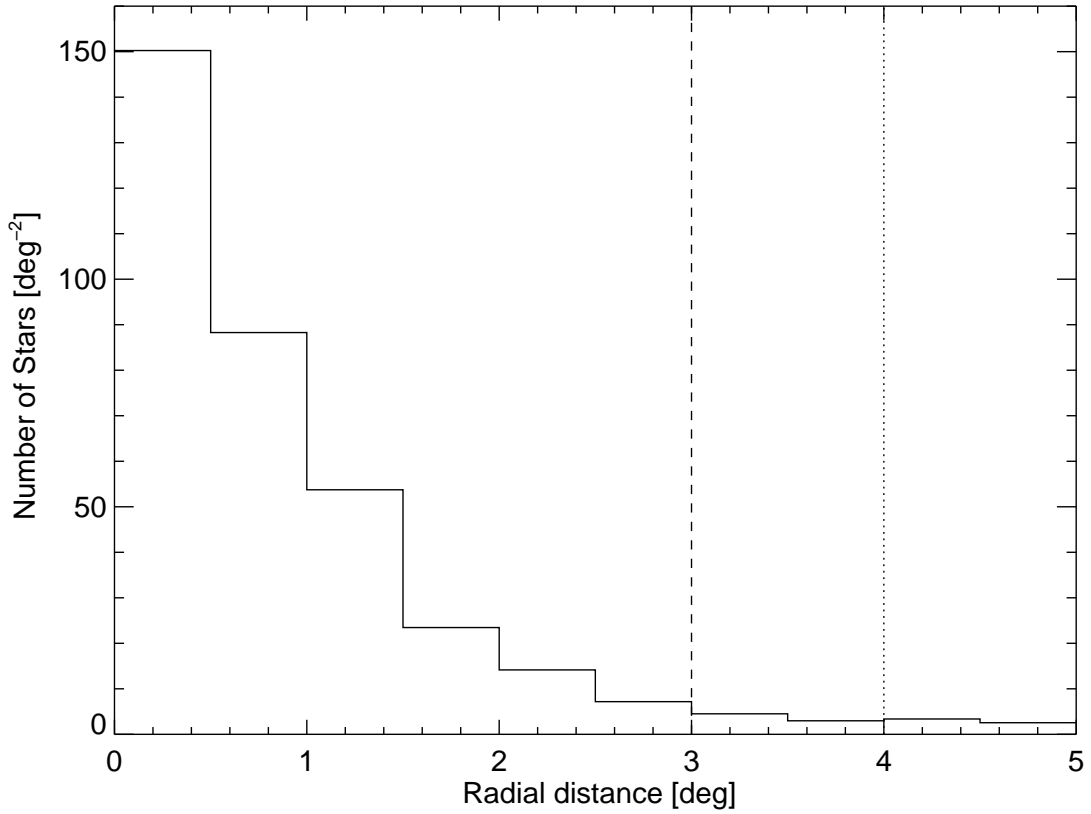[1]Updated to January 2013, available at `http://www.astro.iag.usp.br/$\sim$wilton/`.

Fig. 3.— The radial density distribution of all stars within the entire 5° field satisfying the isochrone and PM criteria. The vertical line at the 3° radius marks where we consider the cluster region in our analysis. The region between radius 4° (shown by another vertical line) and 5° is used as the field region.

the transformation from z_{SDSS} was used, $y_{\text{P1}} = z_{\text{SDSS}} + 0.031 - 0.095\,x$, where x is again $(g-r)_{\text{SDSS}}$. Because of this, plus the Paschen absorption, the transformation to y_{P1} (and to z_{P1}) has a larger uncertainty than in other bands (Tonry et al. 2012a). In the transformation to either g_{P1} or y_{P1}, using the quadratic instead of the linear fit makes little difference. The bottom panel of Figure 4 plots g_{P1} versus $g_{\text{P1}} - y_{\text{P1}}$ together with the PS1 main sequence transformed from Kraus & Hillenbrand (2007). For the PS1/PPMXL sample, the selection range is from 0.15 mag below to 0.4 mag above and perpendicular to the Kraus & Hillenbrand (2007) main sequence transformed to the PS1 system (Tonry et al. 2012a).

The combination of the 2MASS/PPMXL and the PS1/PPMXL samples contains a total of 1040 stars that satisfy all the criteria of photometry (along the isochrone), kinematics (consistent PMs), and spatial (within a 3° radius) grouping. In comparison, there are 168 stars satisfying the identical set of criteria except being with radii between 4° and 5° (which happens to have the same sky area as the 3° cluster radius, i.e., $9\pi\,\text{deg}^2$) — these are considered field stars and this number of stars should be subtracted from the cluster region. So our final list contains 1040 member candidates, among which about 872 ($\sim 84\%$) should be true cluster members. Statistically a brighter candidate is more likely to be a true member than a fainter candidate because of the field contamination. If the stringent criterion of $\Delta\mu = 4$ mas yr^{-1} had been used instead, the number of candidates would have become 547 within 3°, and 33 between 4° and 5°, yielding a net of 514 members within 3°, yielding a 6% false positive rate.

4.   The Updated Member List

Table 1 lists the properties of the 1040 candidates. The first two columns, (1) and (2), are the identification number and coordinates. Columns (3) and (4) give the PM
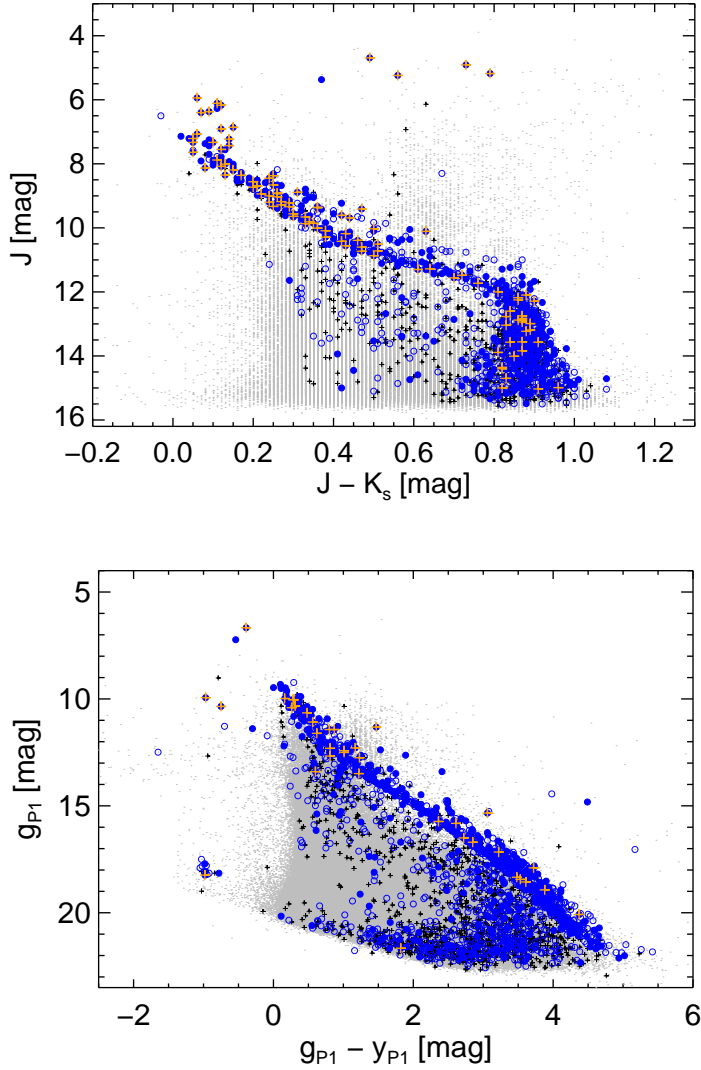
Fig. 4.— Top: The J versus $J - K_s$ CMD for all the stars (gray dots), those with angular distances greater than $3°$ from the cluster center but with $\Delta\mu < 9$ mas yr^{-1} (small black crosses), those within $3°$ from the cluster center and with $\Delta\mu < 9$ mas yr^{-1} (blue open circles), and those within $3°$ and with $\Delta\mu < 4$ mas yr^{-1} (blue filled circles). The stars at the very center of the cluster, namely within $30'$, and with $\Delta\mu < 4$ mas yr^{-1} are highly probable members and are marked as orange crosses. Note the group of blue stragglers beyond the main sequence turn-off point (Andrievsky 1998). Bottom: The g_{P1} versus $g_{P1} - y_{P1}$ CMD, with the same symbols as in the top panel. The group of stars near $g_{P1} = 18$ mag, and $g_{P1} - y_{P1} = -1$ mag include white dwarfs known in the cluster (Dobbie et al. 2004, 2006).

measurements and errors in right ascension and in declination taken from the PPMXL catalog. Subsequent columns, from (5) to (12), list the photometric magnitudes and corresponding errors of PS1 g_{P1}, r_{P1}, i_{P1}, z_{P1}, and y_{P1}, and 2MASS J, H, and K_s. The (13) column flags if the candidate is possibly binary. The last (14) column lists the common star name, if any. The 2MASS and PS1 CMDs of the members listed in Table 1 are displayed in Figure 5, along with a selected stellar models: BT-Settl (Allard et al. 2013; Allard 2014)[2], Siess et al. (2000), Padova (Marigo et al. 2008), and Kraus & Hillenbrand (2007). To convert the effective temperature in the Siess et al. (2000) models to J, H, and K_s magnitudes, we made use of the table presented in Kenyon & Hartmann (1995). While all isochrones follow roughly each other for $J \lesssim 12$ mag, they differ noticeably toward faint magnitudes. The Padova isochrone is too blue to fit the data. This cannot be caused by reddening because Praesepe is very nearby, so is hardly reddened $E(B-V) = 0.027$ mag (Taylor 2006). The rest four stellar models, though diverging toward the lowest mass end of our data, fit the data equally well. The highly secured list of candidates indicates a better fit with the BT-Settl model.

Our member candidates have been selected as grouping in five out of six-dimensional photometric and kinematic parameters, less only the radial velocity measurements. Our list hence is more reliable than using photometry alone, and is comprehensive in terms of stellar mass and sky area coverage than currently available. Among the 1040 candidates, 214 were selected by the 2MASS/PPMXL sample only, 82 by PS1/PPMXL only, and 742 by both. The reason that PS1/PPMXL does not find more candidates is, other than the limit at the bright end, because the faintest candidates are very red, $g_{P1} - K_s \approx 7$ mag — in favor of 2MASS detection — and because the PS1/PPMXL data are limited by the brightness limit

---

[2]`http://perso.ens-lyon.fr/france.allard/`, the latest of NextGen models by Hauschildt et al. (1999) using the solar abundance of Asplund et al. (2009)

Table 1. Member Candidates of Praesepe

No.	R.A. Decl. (J2000)	$\mu_\alpha\,\cos\delta$	μ_δ	g_{P1}	r_{P1}	i_{P1}	z_{P1}	y_{P1}	J	H	K_s	Flag	Remarks
	[deg]	[mas yr^{-1}]	[mas yr^{-1}]	[mag]	[mag]	[mag]	[mag]	[mag]	[mag]	[mag]	[mag]		
(1)	(2)	(3)	(4)	(5)	(6)	(7)	(8)	(9)	(10)	(11)	(12)	(13)	(14)
413	129.7619871 19.7248670	-34.8 ± 1.1	-13.6 ± 1.1	12.120 ± 0.001	...	...	...	...	8.366 ± 0.026	8.126 ± 0.021	8.125 ± 0.021	0	BD+20 2140
414	129.7620587 19.5325438	-37.5 ± 4.1	-16.9 ± 4.1	17.618 ± 0.005	16.347 ± 0.002	15.095 ± 0.600	14.364 ± 0.001	14.060 ± 0.003	12.829 ± 0.022	12.182 ± 0.021	11.962 ± 0.019	1	
415	129.7627808 19.4043081	-38.9 ± 4.1	-16.2 ± 4.1	19.373 ± 0.018	18.124 ± 0.009	16.549 ± 0.003	15.841 ± 0.002	15.494 ± 0.003	14.261 ± 0.027	13.643 ± 0.027	13.407 ± 0.035	1	
416	129.7633143 20.0437781	-44.3 ± 4.1	-13.7 ± 4.1	14.975 ± 0.001	13.827 ± 0.001	13.489 ± 0.600	13.074 ± 0.001	12.927 ± 0.001	11.867 ± 0.023	11.209 ± 0.021	11.051 ± 0.020	0	
417	129.7651196 19.9997784	-31.5 ± 1.1	-12.6 ± 1.3	...	...	...	12.844 ± 0.002	12.690 ± 0.002	7.860 ± 0.023	7.819 ± 0.016	7.769 ± 0.018	0	HD 73430
418	129.7663424 20.5672773	-38.0 ± 4.1	-11.3 ± 4.1	17.691 ± 0.006	16.496 ± 0.003	15.336 ± 0.600	14.615 ± 0.001	14.342 ± 0.002	13.108 ± 0.025	12.464 ± 0.024	12.276 ± 0.021	1	
419	129.7670607 19.5226714	-37.4 ± 4.1	-12.3 ± 4.1	14.274 ± 0.001	13.482 ± 0.600	13.076 ± 0.600	12.831 ± 0.600	12.601 ± 0.001	11.562 ± 0.022	10.987 ± 0.019	10.857 ± 0.016	0	
420	129.7712342 19.7573463	-36.1 ± 4.1	-15.6 ± 4.1	19.064 ± 0.016	17.807 ± 0.009	16.395 ± 0.600	15.616 ± 0.001	15.289 ± 0.003	14.010 ± 0.024	13.424 ± 0.030	13.164 ± 0.028	1	
421	129.7717692 20.1172023	-35.1 ± 1.1	-14.3 ± 1.2	9.489 ± 0.600	9.354 ± 0.600	9.347 ± 0.600	9.375 ± 0.600	9.383 ± 0.600	8.603 ± 0.030	8.455 ± 0.026	8.413 ± 0.027	0	HD 73429
422	129.7754141 19.6768137	-33.7 ± 1.2	-13.9 ± 1.2	7.539 ± 0.600	7.519 ± 0.600	7.559 ± 0.600	7.573 ± 0.600	7.586 ± 0.600	6.857 ± 0.026	6.769 ± 0.023	6.708 ± 0.018	0	HD 73449

Note. — Table 1 is published in its entirety in the electronic edition of the journal. A portion is shown here for guidance regarding its form and content.
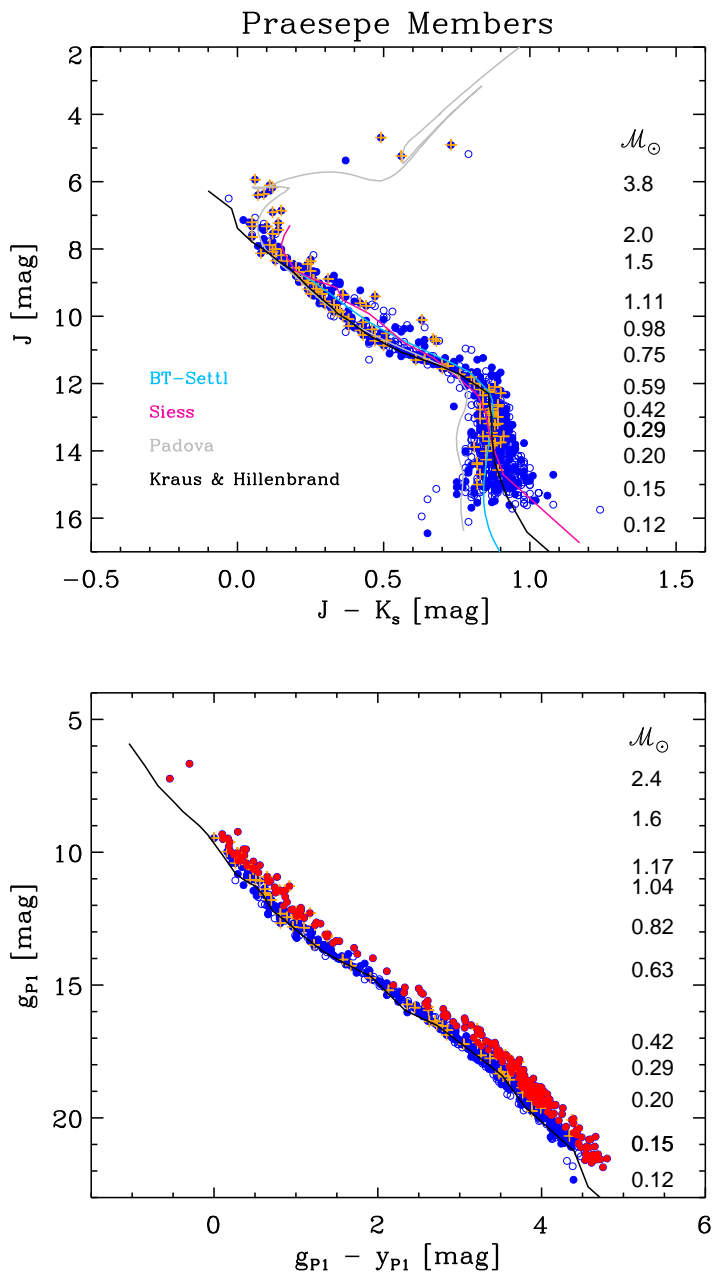
Fig. 5.— Member candidates in Praesepe selected on the basis of position, proper motion, and magnitude/color. Top: The J versus $J - K_s$ CMD, together with the stellar models of BT-Settl (Allard et al. 2013; Allard 2014), Siess, Padova, and Kraus & Hillenbrand (2007). Selected stellar mass values are labeled. Symbols are the same as in Figure 4. Bottom: The g_{P1} versus $g_{P1} - y_{P1}$ CMD for candidates. The solid curve is the main sequence from Kraus & Hillenbrand (2007) transformed to the PS1 system. Red symbols mark possible binaries.

of PPMXL. The situation will improve once PS1 produces its own PM measurements. A total of 890 of our candidates coincide with those by Kraus & Hillenbrand (2007), 567 with those by Boudreault et al. (2012), and 190 with neither. Of the latter, 96 candidates have not been identified in either Hambly et al. (1995b), Pinfield et al. (1997), Adams et al. (2002), or Baker et al. (2010). Some of our candidates missed by Boudreault et al. (2012) are located in the UKIDSS survey gap.

Membership identification by photometry alone, e.g., by González-García et al. (2006) and Boudreault et al. (2010), is vulnerable to significant contamination by field stars, so reliable membership could be secured for bright stars only. To illustrate this, the entire PS1/PPMXL 5° sample contains 320,312 stars. There would have been 2445 candidates if only the photometric and positional criteria were set, but the number reduces drastically to 826 once the additional PM criterion ($\Delta\mu \leq 9$ mas yr^{-1}) is imposed.

Our member list includes the two stars recently reported by Quinn et al. (2012), BD+20 2184 (their Pr 0201=NGC 2632 KW 418) and 2MASS J08421149+1916373 (their Pr 0211=NGC 2632 KW 448), to host exoplanets. A few candidates found in previous works did not pass our PM selection. For example, stars J083850.6+192317 and J084108.0+1914901, listed by González-García et al. (2006) as members on the basis of optical and infrared photometry, have PMs ($\mu_\alpha \cos\delta = 197.5$ mas yr^{-1} and $\mu_\delta = 79.6$ mas yr^{-1} for J083850.6+192317, and $\mu_\alpha \cos\delta = -58.4$ mas yr^{-1} and $\mu_\delta = 24.9$ mas yr^{-1} for J084108.0+1914901) inconsistent with being part of Praesepe. Another highly probable member suggested by González-García et al. (2006), J084039.3+192840, already refuted by Boudreault et al. (2010) because of its $(I_c - K_s)$ color, is indeed not in our candidate list. Of the six brown dwarf candidates proposed by Boudreault et al. (2010, their Table 5), only three are found in our data, though the identification for either stars No. 099, or No. 909 is uncertain because of a nearby star in

each case (see the finding charts in their Fig. 8). Only star No. 910 may have a PPMXL counterpart within $10''$, but it has a proper motion ($\mu_\alpha \cos \delta = -10.5 \pm 7.3 \,\mathrm{mas\,yr^{-1}}$, $\mu_\delta = -10.7 \pm 7.3 \,\mathrm{mas\,yr-1}$) inconsistent with membership. The brown dwarf candidate found by Magazzù et al. (1998), NGC 2632 Roque Praesepe 1, was not in our list because of its faint magnitude ($J = 21.0$ mag).

van Leeuwen (2009) identified, but not tabulated, 24 *Hipparcos* members in Praesepe. With the identifications kindly provided by van Leeuwen, we confirm that they are all enlisted in our candidate sample. The blue stragglers in the cluster suggested by Andrievsky (1998), HD 73666, HD 73819, HD 73618, HD 73210, too bright for PS1, are all confirmed to be PM members. Our photometric selection precludes the white dwarfs known in the cluster (Dobbie et al. 2004, 2006). They are too faint for 2MASS but have been recovered by PPMXL and PS1, illustrated in Figure 4. One additional white dwarf candidate is identified in our data ($\alpha = 127.166145°$, $\delta = +19.728674°$, J2000; $\mu_\alpha = -40.4 \pm 5.2 \,\mathrm{mas\,yr^{-1}}$, $\mu_\delta = -20.4 \pm 5.2 \,\mathrm{mas\,yr^{-1}}$) with $g_{\mathrm{P1}} = 18.15$ mag, and $y_{\mathrm{P1}} = 19.07$ mag. The white dwarf members follow the general cooling sequence from brighter/bluer to fainter/redder in the CMD. Scaled with white dwarfs in the field, studied by Tonry et al. (2012b) also with PS1 data, the ones in Praesepe have a cooling time scale of 0.2–0.4 Gyr.

4.1. Binary Fraction

A binary system with identical component stars would have the brightness of either star overestimated by 0.75 mag. A binary sequence therefore is often seen as a swath up to 0.7–0.8 mag above the main sequence of a star cluster in a CMD. Multiple systems may have even larger magnitude differences. Steele & Jameson (1995) and Hodgkin et al. (1999) estimated a multiplicity of ~ 0.5 for low-mass members in Praesepe. In both the 2MASS and PS1 CMDs (see Figure 5), the binary sequence stands out clearly. Such a

distinct binary sequence was already noticed by Kraus & Hillenbrand (2007). Note that the J versus $J - K_s$ main sequence is characterized by a slanted upper part and turns nearly vertically below the mass of ~ 0.6 M$_\odot$. While the upper main sequence allows us to gauge the distance (shifting vertically), the vertical segment provides a convenient tool to estimate the reddening of a cluster (shifting horizontally). This fact, however, also means the J versus $J - K_s$ CMD cannot be used to evaluate the binarity at the lower main sequence. Instead, the PS1 CMD shows a monotonic track, so is useful for this purpose.

There is no clear dividing line above the main sequence to separate binaries from single stars. The bottom panel of Figure 5 demonstrates a magnitude difference of 0.5 mag above the main sequence as the dividing line. In this case, there are 242 stars above the line, or a binary fraction of about 23% of the total 1040 member candidates. No attempt was made to estimate separately the binarity of the 872 true member versus the 168 interloper samples. If the difference is lower to 0.4 mag or 0.3 mag, the number increases, respectively, to 302 (29%) or 389 (37%). The relatively small increase in the binary fraction is the consequence of a distinct binary sequence of this cluster; that is, the binaries in Praesepe tend to be of similar-mass systems, as noted, for example, by Pinfield et al. (2003). Praesepe also seems to teem with multiple systems, as concluded by Khalaj & Baumgardt (2013). Boudreault et al. (2012) conducted an elaborative analysis on the binarity. Adopting a brightness range from 0.376 to 1.5 mag above the (single star) main sequence, these authors derived a binary frequency of $23.3 \pm 7.3\%$ for the mass range of 0.45 to 0.2 M$_\odot$, $19.6 \pm 3.8\%$ for 0.2 to 0.1 M$_\odot$, and $25.8 \pm 3.7\%$ for 0.1 to 0.07 M$_\odot$. Given the uncertainties in membership and binarity assignments, our data do not justify division of the sample into different mass bins, and we infer an overall binary frequency (or multiplicity) of at least 20–40%.

4.2. Cluster Mass Function

The stellar mass was interpolated via a least-square polynomial fitting to the J (if too bright in PS1) or g_{P1} magnitude using the compilation of Kraus & Hillenbrand (2007) (their Table 5), and adopting a distance modulus of 6.26 mag. The g_{P1} band observations saturate around $g_{P1} \sim 14$ mag, corresponding to $J \sim 11.5$ mag in our sample, or about 0.6 $M_\odot$. The masses of our candidates range from ~ 0.11 $M_\odot$ to ~ 2.39 $M_\odot$.

The luminosity function of the cluster was derived by subtraction of the field contamination. For field stars, we selected the stars satisfying the same PM and isochrone criteria, but with angular distance between $4°$ and $5°$ from the cluster center. In Figure 6, the g_{P1} luminosity function of the member candidates listed in Table 1 is subtracted by that of the field. The field distribution is flat, as expected, and contributes only as a small correction to the observed luminosity function. The corrected luminosity function rises spuriously near the PS1 saturation limit of $g_{P1} \sim 11$–15 mag, and then turns around near $g_{P1} \sim 18$ mag, or mass ~ 0.3 $M_\odot$.

The mass function of Praesepe members is shown in Figure 7. We note that this is the mass function for the stellar systems, i.e., with no binary correction. Using optical I_c band and near-infrared J and K_s photometric data, Boudreault et al. (2010) reported a rising mass function in the range from 0.6 $M_\odot$ to 0.1 $M_\odot$ then turning over, in agreement with previous works, e.g., by Hambly et al. (1995b). This increase in number with decreasing mass was shown by Wang et al. (2011) to continue into the brown dwarf regime, peaking around 70 M_{Jup} then decrease until about 50 M_{Jup}. Kraus & Hillenbrand (2007) and Baker et al. (2010) also derived a rising, but flatter, mass function. On the other hand, Boudreault et al. (2012), using also the UKIDSS photometry, but adding additional proper motion information, obtained an opposite result, namely, a declining mass function between 0.6 $M_\odot$ and 0.1 $M_\odot$, different from those by Hambly et al. (1995b), Chabrier (2005),

Kraus & Hillenbrand (2007), Baker et al. (2010), and Boudreault et al. (2010). Our sample is more complete at the higher mass end than that by Boudreault et al. (2012), but otherwise the mass function is consistent with theirs for stellar masses greater than around 0.3 $M_\odot$. Overall, the mass function we obtained resembles that of the disk population (Chabrier 2005) for the massive part, but shows a deficit of the lowest mass population ($\lesssim 0.3$ $M_\odot$).

4.3. Spatial Distribution of Members

Even the youngest star clusters may have elongated shape (Chen, Chen, & Shu 2004), likely a consequence of filamentary structure in the parental clouds. Subsequent encounters among member stars then circularize the core of a cluster. Mass segregation occurs as energy losing massive stars sink to the center, whereas lower-mass members gain energies and occupy a larger volume in space. Some stars may gain sufficient speed so as to escape the system. The lowest mass members are particularly vulnerable to such stellar "evaporation". As the cluster evolves, the internal gravitational pull becomes weaker and external disturbances, such as differential rotation, or tidal force from passing molecular clouds and from the Galactic disk, act together to distort the shape of a cluster and eventually tear it apart. The deformation and tidal stripping are effective even for globular clusters (Chen & Chen 2010).

Figure 8 shows how the stellar mass correlates with the spatial distribution. The radial density profiles have been computed for four different mass groups: $M/M_\odot \leq 0.2$ (129 stars), $M/M_\odot = 0.2$–0.35 (256 stars), $M/M_\odot = 0.35$–0.7 (332 stars), and $M/M_\odot \geq 0.7$ (323 stars). The top panel shows the observed density profiles, while the bottom panel compares the normalized profiles. Because of the normalization, no correction of the field contamination is necessary. Relatively massive members appear to be centrally concentrated, whereas
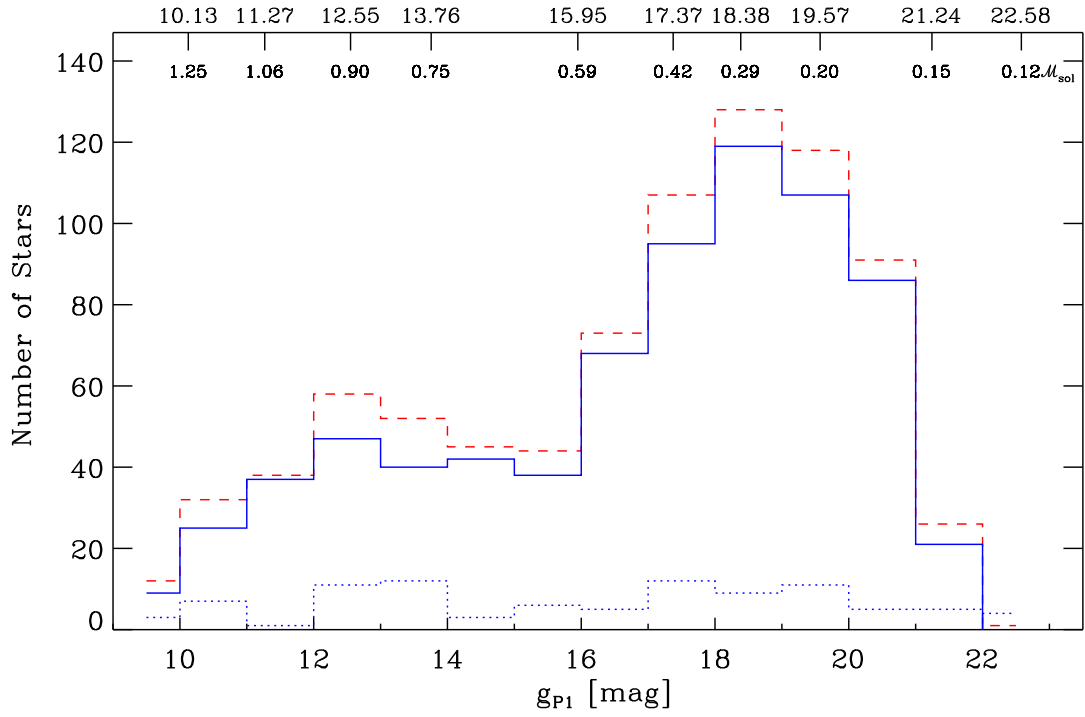
Fig. 6.— The observed g_{P1} luminosity function of member candidates (the red dash line) is subtracted by the field population with the same photometric and PM selection criteria (blue dotted line) to derive the corrected cluster luminosity function (solid blue line). The corresponding stellar mass is labeled at the top in unit of solar mass.
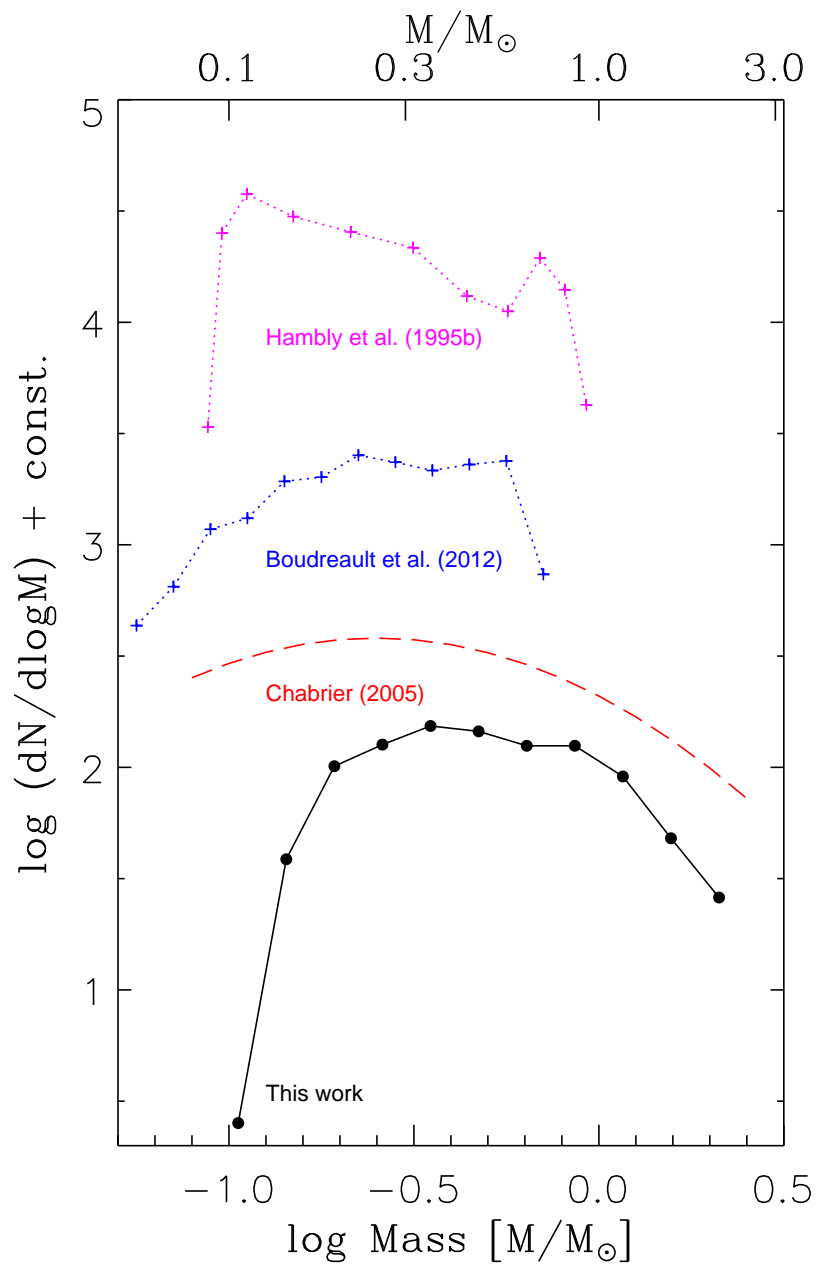
Fig. 7.— The mass function of Praesepe (solid line). Also shown are that by Chabrier (2005) for the disk population (long-dashed line), and those by Hambly et al. (1995b) (a representative rising mass function) and Boudreault et al. (2012) (representing a falling mass function) for Praesepe (dashed lines), each shifted vertically for display clarity.

lower mass members are more scattered spatially, a result of mass segregation.

Mass segregation in Praesepe was well demonstrated already by Hambly et al. (1995b), Kraus & Hillenbrand (2007), and Khalaj & Baumgardt (2013). Our result is consistent with that by Hambly et al. (1995b) from 0.85 $M_\odot$ to 0.15 $M_\odot$. When the radial density distribution shown in Figure 8 is parameterized with an exponential form, $\sigma(r) \propto e^{-\alpha r}$, the least-squared fitting yields $\alpha = 2.21$ (for members > 0.7 $M_\odot$), 0.96 (0.35–0.7 $M_\odot$), and 0.42 (0.2–0.35 $M_\odot$). Caballero (2008) suggested that a power-law function may be more appropriate. In any case, for the faintest sample, the density distribution is certainly not exponential. Instead, it exhibits a sharp truncation beyond $1°$. We interpret this as a consequence of stellar evaporation. This further supports the notion of a relative lack of low-mass stars in Praesepe, as already demonstrated in Figure 7.

Mass segregation is further manifested by the positional (Figure 9) and PM distributions (Figure. 10) of the members; namely, relatively massive members are concentrated in a smaller volume in space, and have a smaller velocity dispersion than lower-mass stars. The average stellar mass in our sample is $\bar{m} \approx 0.59$ $M_\odot$, close to that for a Miller-Scalo initial mass function. With the total number of members $N = 872$, the total stellar mass in the cluster then amounts to at least ~ 520 $M_\odot$. The lowest mass stars, with a declining mass function, do not contribute significantly to the total mass. With a radius $R = 9$ pc, the velocity dispersion of the cluster then would be $v \approx (GN\bar{m}/R)^{1/2} = 0.5$ km s^{-1}, which is noticeably less than the typical value of 1–2 km s^{-1} for Galactic open clusters. At the assumed distance of 179 pc to Praesepe, an intracluster PM dispersion of 1 mas yr^{-1} corresponds to a velocity dispersion of 0.8 km s^{-1}. Our data thus are not precise enough to measure any PM gradient among members.

The evidence is mounting that Praesepe is dissolving. It is spatially extended with a sparse stellar density. Holland et al. (2000) suggested that Praesepe might consist of

two merging clusters. The relatively high fraction of equal mass pairs (and of multiples) may be the consequence of occasional stellar ejection during three-body encounters (Binney & Tremaine 1987), or during the merging process. Relevant time scales for a dissolving star cluster include: (i) the dynamical (crossing) time scale, $\tau_{\rm dyn} \approx 2R/v$, ($ii$) the relaxation time, $\tau_{\rm relax} \approx \tau_{\rm dyn}\,0.1\,N/\ln N$, and (iii) the evaporation time, $\tau_{\rm evap} \approx 100\,\tau_{\rm relax}$ (Binney & Tremaine 1987). For Praesepe, these time scales are $\tau_{\rm dyn} = 3.6 \times 10^7$ yr, $\tau_{\rm relax} = 4.6 \times 10^8$ yr, and $\tau_{\rm evap} = 4.6 \times 10^{10}$ yr, respectively. The lowest-mass members, having an average escape probability (Spitzer 1987) several times of that for the most massive stars, are particularly susceptible to ejection. The Praesepe cluster therefore is almost fully relaxed, and tidal stripping has occurred, starting with the lowest mass members being witnessed to escape from the cluster.

5.   Summary

We have conducted a photometric and proper motion selection of member stars of the Galactic open cluster Praesepe, using 2MASS, PPMXL and Pan-STARRS data. Our sample is comprehensive in terms of sky area (3° radius), limiting magnitude ($g_{\rm P1} \sim 21$ mag), and reliability ($\sim 16\%$ false positive rate). A total of 1040 member candidates are identified, 872 of which are highly probable members, down to about 0.1 solar masses. While for members more massive than 0.6 $\rm M_\odot$, the Padova isochrone works well, the BT-Settl atmospheric model fits better toward fainter magnitudes. The binary frequency of Praesepe members is about 20–40%, with a relatively high occurrence of similar mass pairs. The mass function is consistent with that of the disk population, but with a deficit of stars less massive than 0.3 $\rm M_\odot$. Members show a clear evidence of mass segregation, with the lowest mass population being evaporated from the system. At the faint magnitude end, the bottleneck of membership selection for very faint objects remains the sensitivity of the PM
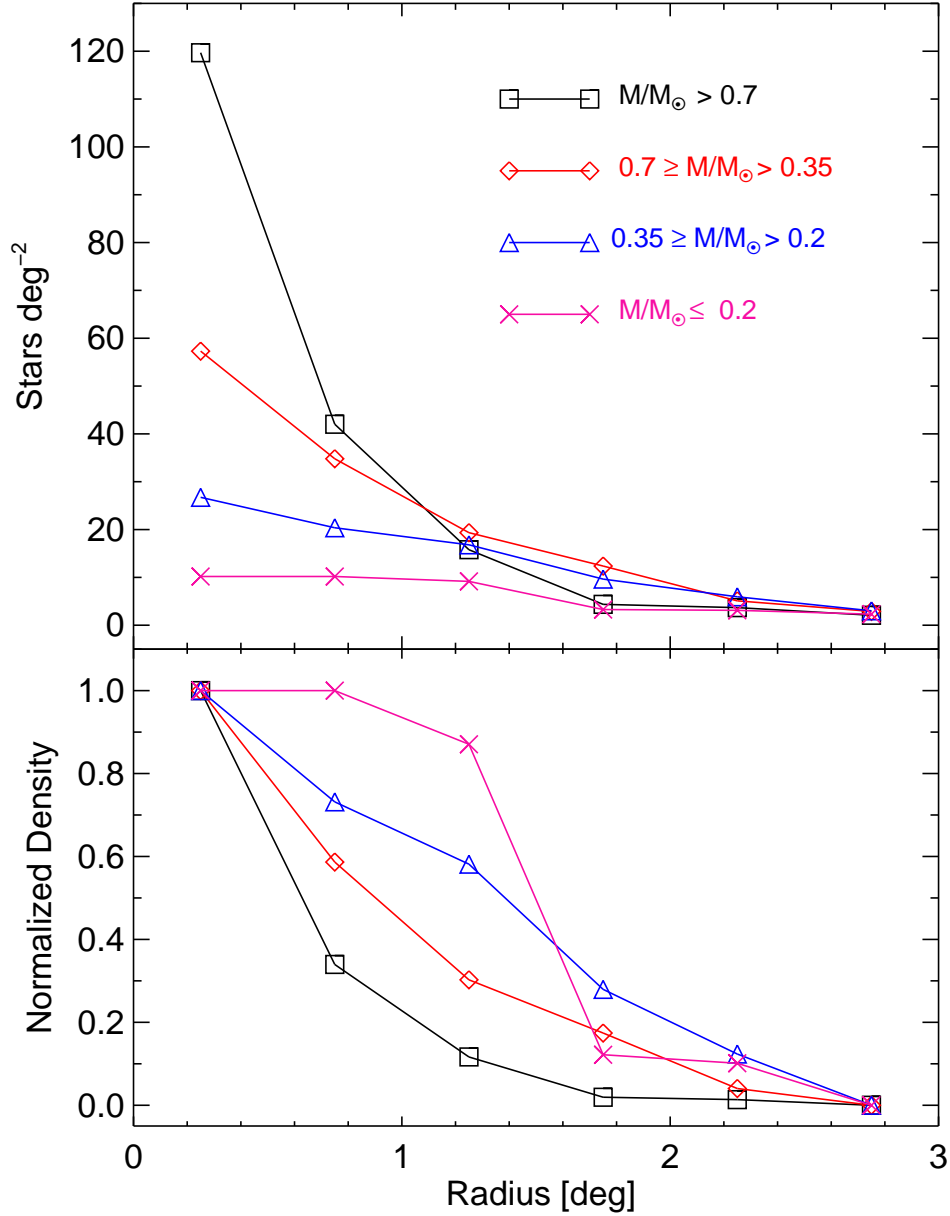
Fig. 8.— The radial density distribution of the members. The lines with different colors show different magnitude ranges. The top panel shows each derived distribution and the bottom panel shows the same but normalized from unity at the center to zero at the edge of the cluster.
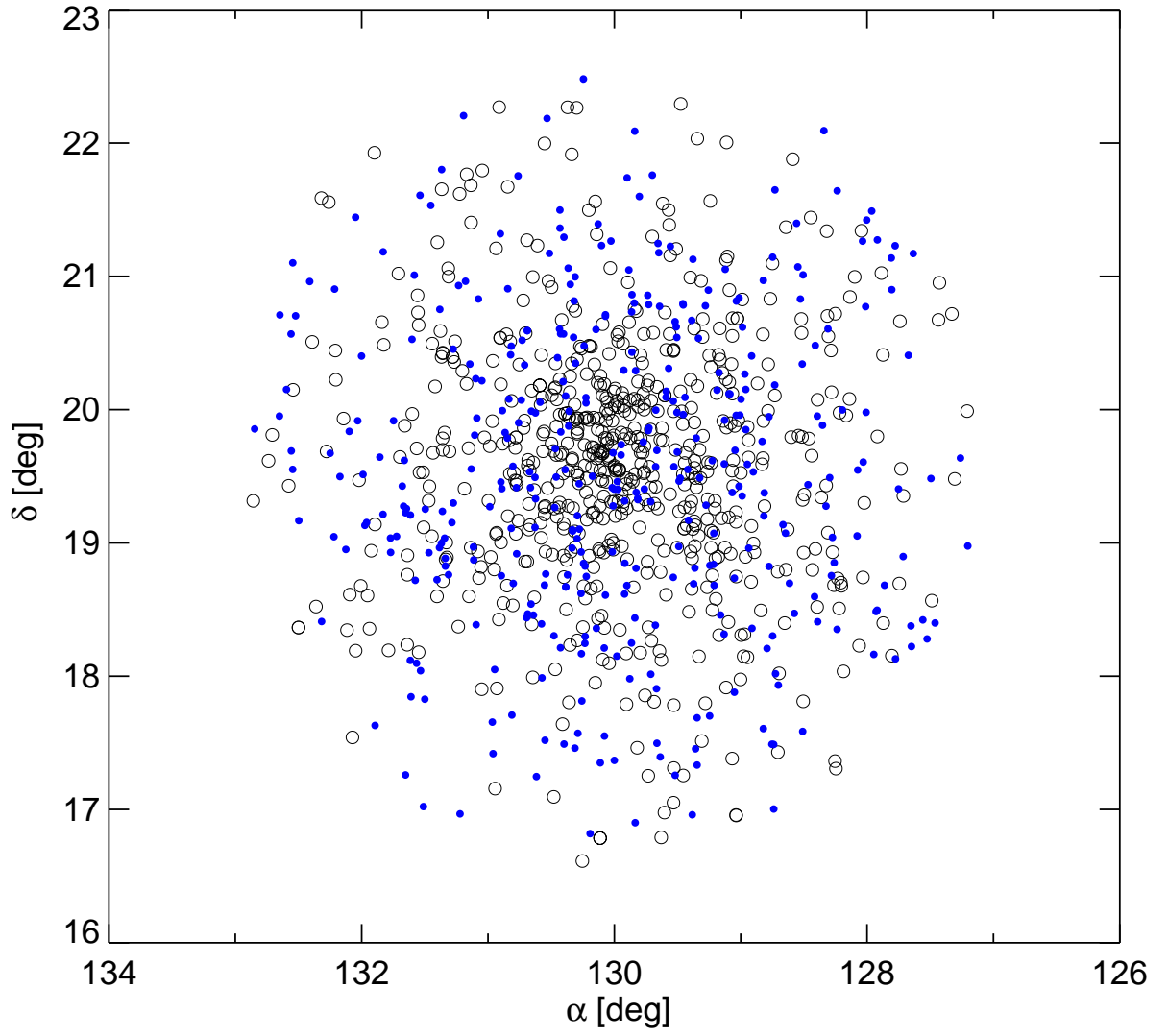
Fig. 9.— Positional distributions of stars more massive (open circles) and less massive (solid circles) than 0.35 M$_\odot$.
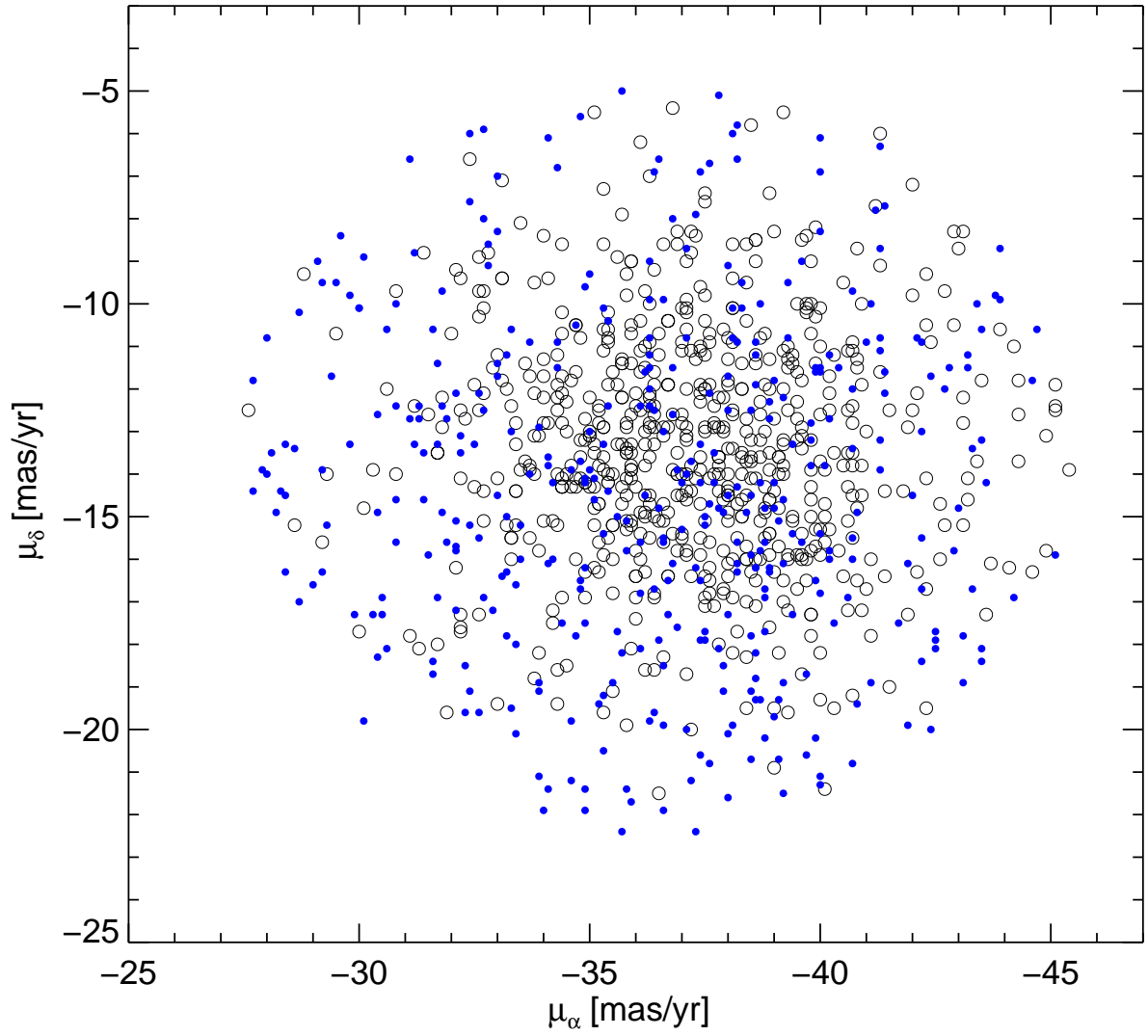
Fig. 10.— Proper motion distributions for the same two mass groups of members as shown in Fig. 9.

measurements. Once the PS1 completes its survey in early 2014, increasing the photometric depth and the stellar PM baseline to more than 3.5 years, we expect to secure member lists for nearby star clusters well into the substellar regime.

REFERENCES

Abazajian, K. N., Adelman-McCarthy, J. K., Agüeros, M. A., et al. 2009, ApJS, 182, 543

Adams, J. D., Stauffer, J. R., Skrutskie, M. F., et al. 2002, AJ, 124, 1570

Ahumada, J., & Lapasset, E. 1995, A&AS, 109, 375

An, D., Terndrup, D. M., Pinsonneault, M. H., Paulson, D. B., Hanson, R. B.,& Stauffer, J. R. 2007, ApJ, 655, 233

Allard, F., Homeier, D., & Freytag, B. 2013, Mem. Soc. Astron. Italiana, 84, 1053

Allard, F. 2014, IAU Symposium, 299, 271

Andrievsky, S. M. 1998, A&A, 334, 139

Asplund, M., Grevesse, N., Sauval, A. J., & Scott, P. 2009, ARA&A, 47, 481

Baker, D. E. A., Jameson, R. F., Casewell, S. L., et al. 2010, MNRAS, 408, 2457

Baraffe, I., Chabrier, G., Allard, F., & Hauschildt, P. H. 1998, A&A, 337, 403

Binney, J., & Tremaine, S. 1987, Galactic Dynamics, Princeton, NJ, Princeton University Press, 1987

Boudreault, S., Bailer-Jones, C. A. L., Goldman, B., Henning, T., & Caballero, J. A. 2010, A&A, 510, A27

Boudreault, S., Lodieu, N., Deacon, N. R., & Hambly, N. C. 2012, MNRAS, 426, 3419

Boudreault, S., & Lodieu, N. 2013, MNRAS, 434, 142

Bouvier, J., Kendall, T., Meeus, G., et al. 2008, A&A, 481, 661

Caballero, J. A. 2008, MNRAS, 383, 375

Carrera, R., & Pancino, E. 2011, A&A, 535, A30

Chabrier, G. 2005, in The Initial Mass Function 50 Years Later, Eds. E. Corbelli and F. Palle (Springer, Dordrecht) Ap&SSL, 327, 41

Chappelle, R. J., Pinfield, D. J., Steele, I. A., Dobbie, P. D., & Magazzù, A. 2005, MNRAS, 361, 1323

Chen, W. P., Chen, C. W., & Shu, C. G. 2004, AJ, 128, 2306

Chen, C. W., & Chen, W. P. 2010, ApJ, 721, 1790

de la Fuente Marcos, R., & de la Fuente Marcos, C. 2000, Ap&SS, 271, 127

Dias, W. S., et al. 2002, A&A, 389, 871

Dobbie, P. D., Pinfield, D. J., Napiwotzki, R., et al. 2004, MNRAS, 355, L39

Dobbie, P. D., Napiwotzki, R., Burleigh, M. R., et al. 2006, MNRAS, 369, 383

Eggen, O. J. 1960, MNRAS, 120, 540

Fossati, L., et al. 2008, A&A, 483, 891

Gáspár, A., Rieke, G. H., Su, K. Y. L., et al. 2009, ApJ, 697, 1578

Girard, T. M., Grundy, W. M., López, C. E., & van Altena, W. F. 1989, AJ, 98, 227

González-García, B. M., Zapatero Osorio, M. R., Béjar, V. J. S., et al. 2006, A&A, 460, 799

Hambly, N. C., Steele, I. A., Hawkins, M. R. S., & Jameson, R. F. 1995a, A&AS, 109, 29

Hambly, N. C., Steele, I. A., Hawkins, M. R. S., & Jameson, R. F. 1995b, MNRAS, 273, 505

Hauschildt, P. H., Allard, F., & Baron, E. 1999, ApJ, 512, 377

Hodapp, K.W., Siegmund,W. A., Kaiser, N., et al. 2004, Proc. SPIE, 5489, 667

Hodgkin, S. T., Pinfield, D. J., Jameson, R. F., et al. 1999, MNRAS, 310, 87

Høg, E., Fabricius, C., Makarov, V. V., et al. 2000, A&A, 355, L27

Holland, K., Jameson, R. F., Hodgkin, S., Davies, M. B., & Pinfield, D. 2000, MNRAS, 319, 956

Jones, B. F., & Cudworth, K. 1983, AJ, 88, 215

Jones, B. F., & Stauffer, J. R. 1991, AJ, 102, 1080

Kaiser, N., et al. 2010, Proc. SPIE, 7733, 77330E

Khalaj, P., & Baumgardt, H. 2013, MNRAS, 434, 3236

Klein Wassink, W. J. 1927, Pub. of the Kapteyn Astron. Laboratory Groningen, 41, 1

Kenyon, S. J., & Hartmann, L. 1995, ApJS, 101, 117

Kraus, A. L., & Hillenbrand, L. A. 2007, AJ, 134, 2340

Loktin, A. V., & Beshenov, G. V. 2003, Astron. Rep., 47, 6

Magazù, A., Rebolo, R., Zapatero Osorio, M. R., Martín, E. L., & Hodgkin, S. T. 1998, ApJ, 497, L47

Magnier, E. A., Schlafly, E., Finkbeiner, D., et al. 2013, ApJS, 205, 20

Marigo, P., Girardi, L., Bressan, A., et al. 2008, A&A, 482, 883

Mermilliod, J.-C., Weis, E. W., Duquennoy, A., & Mayor, M. 1990, A&A, 235, 114

Muench, A. A., Lada, E. A., Lada, C. J., & Alves, J. 2002, ApJ, 573, 366

Pinfield, D. J., Hodgkin, S. T., Jameson, R. F., Cossburn, M. R., & von Hippel, T. 1997, MNRAS, 287, 180

Pinfield, D. J., Dobbie, P. D., Jameson, R. F., et al. 2003, MNRAS, 342, 1241

Quinn, S. N., White, R. J., Latham, D. W., et al. 2012, ApJ, 756, L33

Reglero, V., & Fabregat, J. 1991, A&AS, 90, 25

Roeser, S., Demleitner, M., & Schilbach, E. 2010, AJ, 139, 2440

Siess, L., Forestini, M., & Dougados, C. 1997, A&A, 324, 556

Siess, L., Dufour, E., & Forestini, M. 2000, A&A, 358, 593

Skrutskie, M. F., Cutri, R. M., Stiening, R., et al. 2006, AJ, 131, 1163

Spitzer, L., Jr., & Shull, J. M. 1975, ApJ, 201, 773

Spitzer, L. 1987, "Dynamical Evolution of Globular Clusters", Princeton, NJ, Princeton University Press, 1987

Steele, I. A., & Jameson, R. F. 1995, MNRAS, 272, 630

Taylor, B. J. 2006, AJ, 132, 2453

Tonry, J. L., Burke, B. E., Isani, S., Onaka, P. M., & Cooper, M. J. 2008, Proc. SPIE, 7021, 702105

Tonry, J. L., Stubbs, C. W., Lykke, K. R., et al. 2012, ApJ, 750, 99

Tonry, J. L., Stubbs, C. W., Kilic, M., et al. 2012, ApJ, 745, 42

van Leeuwen, F. 2007, A&A, 474, 653

van Leeuwen, F. 2009, A&A, 497, 209

Wang, J. J., Chen, L., Zhao, J. H., & Jiang, P. F. 1995, A&AS, 113, 419

Wang, W., Boudreault, S., Goldman, B., et al. 2011, A&A, 531, A164

Williams, D. M., Rieke, G. H., & Stauffer, J. R. 1995, ApJ, 445, 359